Research Article

WIND ENGINEERING

Wind Engineering
2022, Vol. 46(2) 392–412

DOI: 10.1177/0309524X211030186
journals.sagepub.com/home/wie
SAGE

Real time implementation of interval type-2 fuzzy logic based damping controller for wind integrated power system

Kanasottu Anil Naik

Abstract

In this paper, the real time simulation results using an interval type-2 fuzzy logic based damping controller of wind integrated power system is presented. The fundamental control block of the employed SATCOM includes the proposed damping controller to reduce the damping oscillations/fluctuations. Real time digital simulations (RTDS) are developed using OPAL-RT real time simulator in order to show the effectiveness of the proposed fuzzy control technique. The real time simulator (RTS) lab consists of two targets (processors). On first processor (target one) a typical wind power system has been implemented and on second processor an interval type-2 fuzzy logic algorithm is modelled and developed hence, hardware in loop (HIL) configuration is achieved. To evaluate the effectiveness of the proposed method by comparative analysis, three different scenarios (STATCOM-without damping controller, STATCOM-with type-1 FLC based damping controller and STATCOM-with interval type-2 FLC based damping controller) are considered subjected to various disturbances such as noise in wind speed and different types of network faults.

Keywords

Wind farm, stability, damping controller, STATCOM, interval type-2 fuzzy logic controller, faults, uncertainties, noise wind speed, fluctuations

Introduction

Recently, wind energy is gaining attention as sustainable energy since it highly eco-friendly, resulting in deep reductions in greenhouse gas emission with low cost of required energy. Several organizations such as American Wind Energy Association (AWEA), National Renewable Energy Laboratory (NREL), and Global Wind Energy Council (GWEC) are working in the world in the area of wind energy research. Recently, GWEC reported that wind energy can provide approximately12% of wind power to the global total electricity demand. Currently, all over the world more than 341,320 wind turbines are spinning (Singh and Sundaram, 2020, 2021; Singh et al., 2019b; The Global Wind Energy Council Belgium, 2020).

There exist two types of wind turbine generator systems which are commercially available – Fixed-speed and variable-speed wind energy systems. In the early stage of wind energy market, the most of wind power systems were employed with fixed speed induction generators (FSIGs) and, still exist due to their low cost, low maintenance and robustness. At present, 20% of the installed wind power is still being produced by squirrel cage induction generator (SCIG) based fixed speed wind energy system (WES). Respectively, in Australia, Germany and Denmark about 87, 48 and 47.1 MW of installed wind turbines (rated 1.5 MW) are SCIG based wind turbines (The Wind power, 2019).

Department of Electrical Engineering, NIT Warangal, Telangana, India

Corresponding author:
Kanasottu Anil Naik, Department of Electrical Engineering, NIT Warangal, Telangana, India.
Email: anilnaik205@nitw.ac.in

However, SCIG based wind farm extremely sensitive to network faults as its stator winding is directly connected to power grid leads to wind farm power fluctuations. These inherent power fluctuations have adverse impacts on the power system to which wind-farm connected (Singh et al. 2018, 2019a, 2020). Moreover, wind speed is intermittent in nature, implying that wind farm output power varies in certain range, therefore, the operating point of power system changes from time to time when the wind energy system integrated to the grid. Much of literature addressed the reduction of power fluctuations in wind integrated power system. Usually, a pitch-angle controller is employed to limit the aerodynamic power at rated level which in addition, can also improve the transient stability of the wind integrated power system (Jauch et al., 2007; Thet and Saitoh, 2009). According to some reports, Breaking Resistors (BR) can be employed for stabilization of induction generator (Causebrook et al., 2007; Ghazi and Aliabadi, 2010). Recently, Superconducting Magnetic Energy System (SMES) has also been employed for grid connected wind generator stabilization (Sheikh et al., 2012). Moreover, in the event of faults, the Superconducting Fault Current Limiter (SFCL) can suppress short-circuit current thereby, it can improve transient stability of induction generator (Ou et al., 2015). (Tan et al., 1993) employed SVC for voltage support and for transient stability improvement by providing sufficient reactive power to the generator during its acceleration. However, STATCOM performs better than the SVC for a given contingency if the same rating devices are assumed (Molinas et al., 2008).

Therefore, in all aspects STATCOM suits well for wind farms, in comparison to other methods. Therefore, in recent time STATCOM has been employed to enhance the transient stability of induction generator (Edrisian et al., 2015; 2012; Sravanthi et al., 2014; Vimalraj et al., 2014) by recovering the voltage effectively. In this trend, some literatures have employed control techniques such as linear damping controllers and state feedback control methods for STATCOM, in order to reduce the power oscillations (Elsamahy et al., 2014). However, recent studies have proposed external damping controller for the STATCOM where it designed using intelligent control techniques such as fuzzy logic, hybrid (fuzzy-PI), and neuro-fuzzy (Ou et al., 2017; Truong, 2016; Wang and Truong, 2013). The fuzzy logic controllers (called as type-1 FLC) are good at reference tracking and exhibit improved system performance in comparison to other controller methods. However, the expert knowledge that is used to construct the rules in a type-1 FLC is uncertain as the knowledge possessed by different experts may not be the same (Mendel, 1999). Therefore, the uncertainty involved in the fuzzy rules and membership functions lead to poor controller performance. Moreover, the uncertainties in actual degree of membership functions (MFs) cannot be modelled once the membership functions have been defined for designing the controller (Hagras and Wagner, 2012).

Acknowledging the limitations of type-1 FLC called as traditional fuzzy logic controller one need to look for the appropriate control technique. Therefore, this work proposed an interval type-2 FLC for external damping controller design of STATCOM and deal with the issues of uncertainty in MFs and fuzzy rules. The type-2 fuzzy logics sets are defined with three dimensional membership function (MF) it includes footprint-of-uncertainty (FOU) (Mendel et al., 2006; Qilian and Mendel, 2000). Due to third dimensional membership function present in the interval type-2 fuzzy logic controller (IT2-FLC), it can over the uncertainties encounter in the fuzzy rules and membership functions. As the wind power system highly uncertain can utilize this special feature of IT-2 FLC very effectively, thereby type-2 FLC based damping controller including with STATCOM control block improve its operational efficiency.

In view of the above, the objectives of this paper are:

(i) Designing of interval type-2 fuzzy logic technique for damping controller which includes in the STATCOM control block.
(ii) Real time implementation of proposed strategy is realized using OPAL-RT platform and hardware in loop (HIL) was developed for rapid control prototyping of the proposed technique.
(iii) Assessment of impact of proposed control technique with varying wind speed considering wind speed noise.
(iv) Investigation of effectiveness of proposed control scheme under network faults in comparison with other conventional control techniques.

Studied system configuration

In this work, a typical wind integrated power system is considered which as shown in Figure 1, it consists of 24 1.5 MW rated fixed-speed SCIGs and thus 36 MW wind farm represented by an equivalent aggregated SCIG driven by an equivalent aggregated fixed-speed WT. The stator winding of the generator is connected at the point-of-

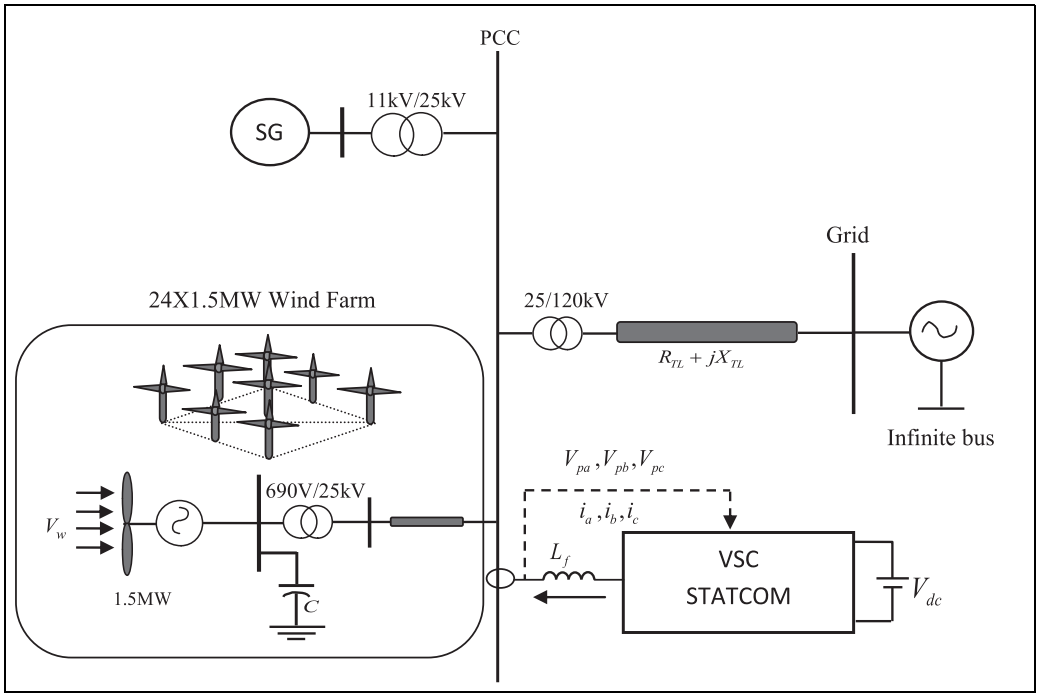

Figure 1. Studied wind farm integrated power system.

common-coupling (PCC) through a step-up transformers (0.69/25 kV) which thereafter, another step-up transformer (25/250 kV) is connected at the PCC which helps in exporting power to the 120 kV grid through a transmission line. To supply the adequate reactive power and voltage support at the PCC, the STATCOM has been employed and connected at the 25 kV bus. A synchronous generator (SG) of 100 MVA is also considered and it get connected to the PCC point from where the wind farm and STATCOM are integrated. The design parameters of the synchronous generator, wind generator, wind turbine and STATCOM are presented in Supplemental Appendix.

Aerodynamic characteristics of wind turbine

The variable wind speed acting as an input to the wind turbine and by rotating blades the mechanical power is developed. Therefore, the extracted mechanical power can be expressed as

$$P_m = 0.5\rho A_r C_p(\lambda, \beta) {V_w}^3 \tag{1}$$

where, ρ is air-density [kg/m^3],A_r is the turbine swept area [m^2] and can be written as $A_r = \pi R^2$, V_w is the wind speeds [m/s] and C_p is the power coefficient and it is a function of pitch angle (β) and tip speed ratio (λ).

Therefore, C_p can be defined as (Ackermann, 2005):

$$C_p(\lambda, \beta) = c_6\lambda + e^{-c_5/\lambda_i}(-c_4 - c_3\beta + c_2/\lambda_i)c_1 \tag{2}$$

where

$$\frac{1}{\lambda_i} = \frac{1}{0.008\beta + \lambda} - \frac{0.035}{1 + \beta^3} \tag{3}$$

Finally, tip speed ration can be expressed as:

$$\lambda = \frac{\omega_r R}{V_w} \tag{4}$$

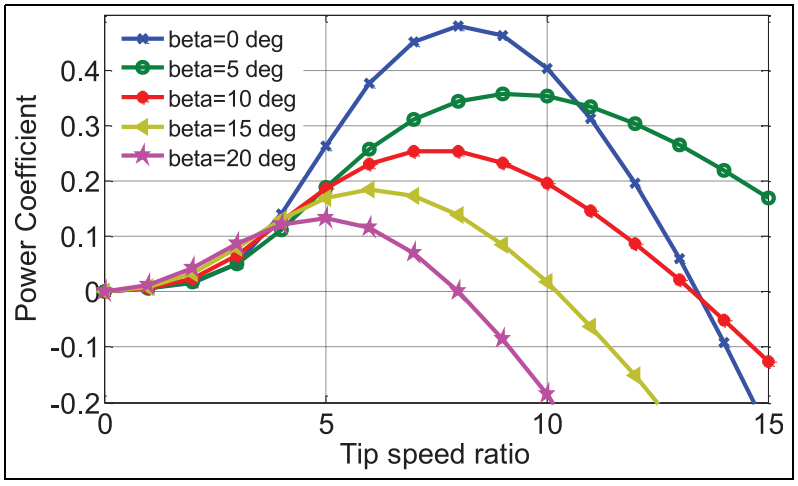

Figure 2. Wind turbine $C_p - \lambda$ curve.

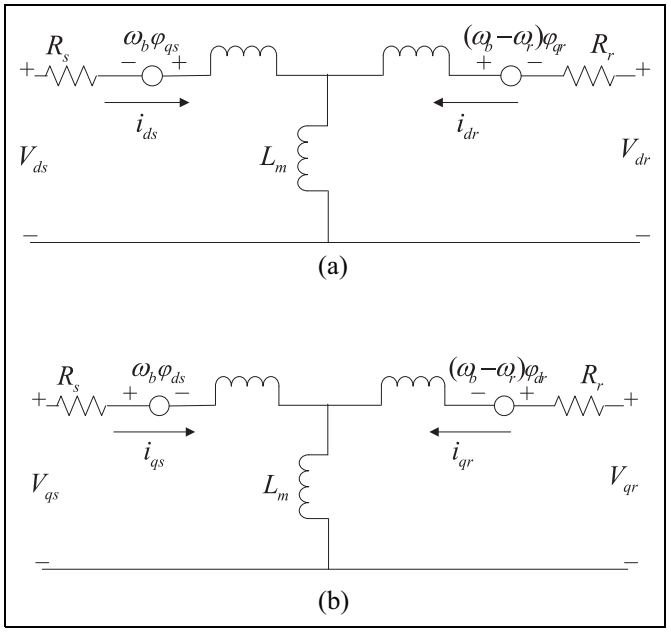

Figure 3. d-q reference frame of the IG (a) d-axis and (b) q-axis.

According to equations (1)–(4), for different values of pitch-angle (β), the powers coefficient versus tip-speed ratio ($C_p - \lambda$) curve for the studied system has been obtained as shown in Figure 2

Induction generator modelling

The a-b-c reference frame of induction generator (IG), is transformed into the *d-q* axis reference frame and the equivalent model is as shown in Figure 3 (Ackermann, 2005). All electrical variables and parameters are referred to the stator.

The electromagnetic torque of the machine can be expressed as:

$$T_e = \varphi_{ds} i_{qs} - \varphi_{qs} i_{ds} \tag{5}$$

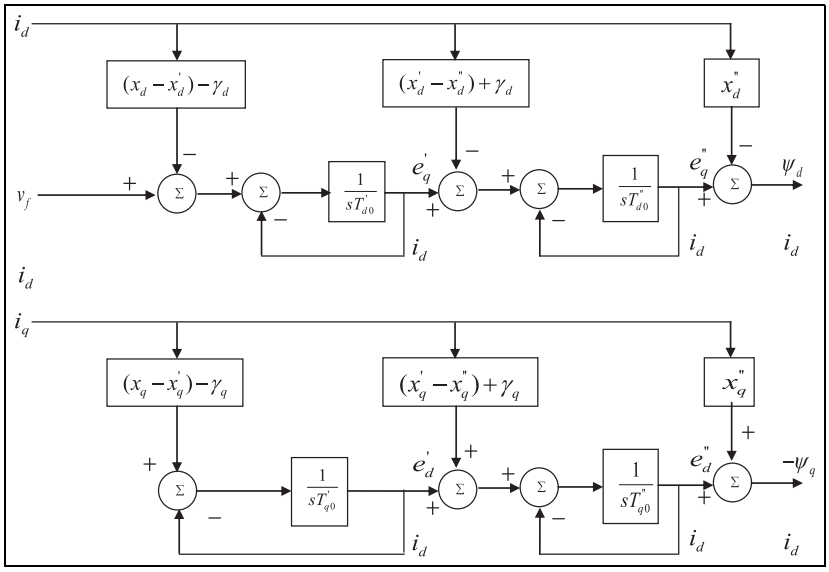

Figure 4. Block diagram representation of SG.

The dynamic equation of motion which represents the equivalent mass of wind turbine and generator rotor can be written as.

$$p\omega_m = \frac{\omega_b}{2H}(T_m - T_e) \tag{6}$$

Where, H is the equivalent inertia constant of both induction generator rotor and wind turbine.

Modelling of synchronous generator

Practically, the Park's 'two reaction theory' of synchronous machine model is used in power system studies. Thus, the fundamental assumptions considered for modelling of a synchronous generator (SG) are well known and are not repeated here (Ackermann, 2005). The system model has been developed by reducing the SG equations in an appropriate form and then combining them with the network equations. The complete d-axis and q-axis studied of SG model is depicted in Figure 4.

STATCOM control scheme

A schematic diagram of a typical STATCOM is as shown in Figure 5 which includes a voltage source converter (VSC), AC filtering inductor and the associated control system. The well-known control scheme (Singh et al., 2006) is used as a control strategy for the VSC based STATCOM.

The voltage regulation controller (PI_{AC}) output (I_q^*) determines the amount of reactive power to be generated by STATCOM, where it reacts to a sudden voltage variation and inject the appropriate amount of reactive power.

At the same time, STATCOM dc bus voltage is supported by another controller i.e.PI_{DC}, here, dc bus voltage (V_{dc}) is compared with the reference dc voltage (V_{dcref}) and the error signal (ΔV_{DC}) passes through it. The output (I_d^*) of this controller determine the source current active power component so that no real power injection is made by STATCOM at the PCC.

STATCOM with damping controller

The control block diagram of damping controller with STATCOM control scheme is shown in Figure 6. Here, STATCOM damping controller utilizes synchronous generator rotor speed deviation (difference between measured SG speed and reference SG speed) as feedback signal to damping controller since it is easier to obtain in practice by measurement and analysis. However, designing a robust damping controller for effective power oscillations

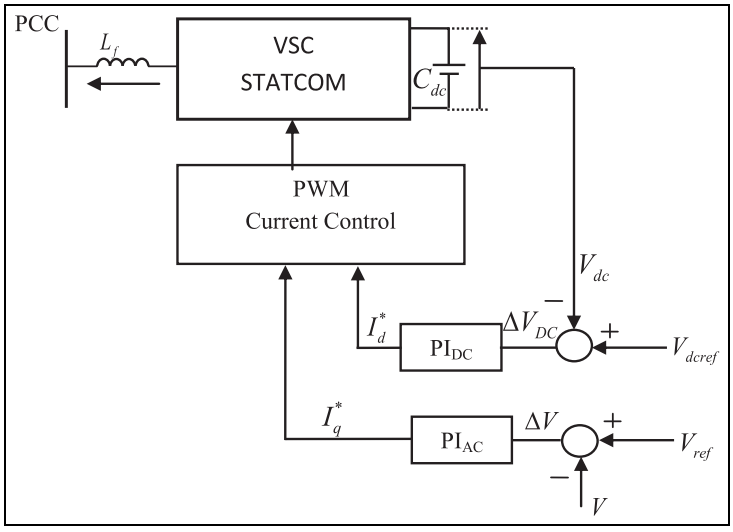

Figure 5. Control scheme of STATCOM.

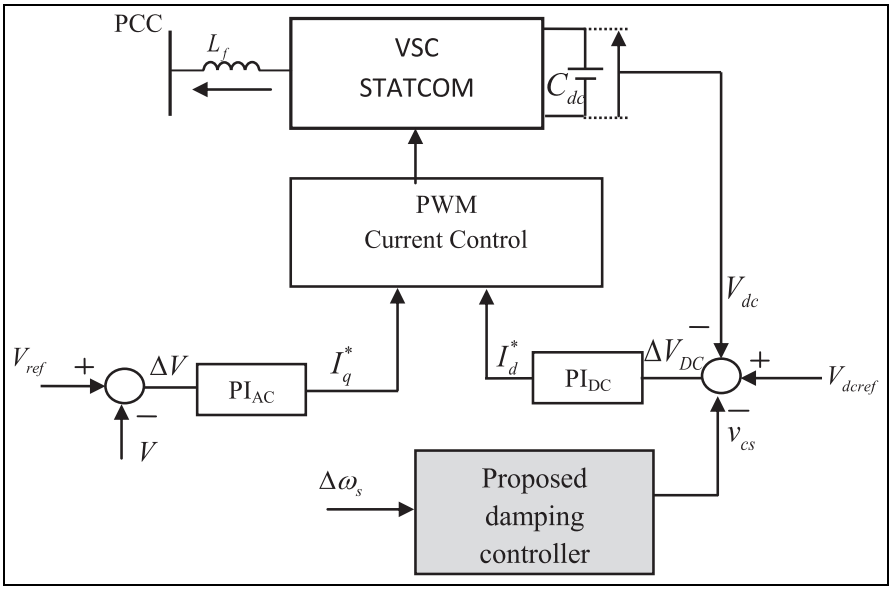

Figure 6. Control block diagram of STATCOM with damping controller.

damping and smooth grid interaction operation subjected to network faults is a challenging task to the control engineers. In response to this challenge, this paper mainly proposes a novel control strategy with interval type-2 fuzzy sets for damping controller of STATCOM, for handling the uncertainties in the network operating conditions. The concept of type-2 FLC is developed from the traditional fuzzy logic (type-1 FLC). It is being assumed that the concept of the type 1 FLC is clear and discussed here in brief.

Type-1 fuzzy logic system

The concept of fuzzy logic (FL) is introduced by Professor Lofty Zadeh in the year1965 (Zadeh, 1965). The objective of the FL is to develop the outputs by using set of membership function rather than crisp value. It has been found to be an excellent choice for many control application as it mimics the human control logic. The fuzzy rules

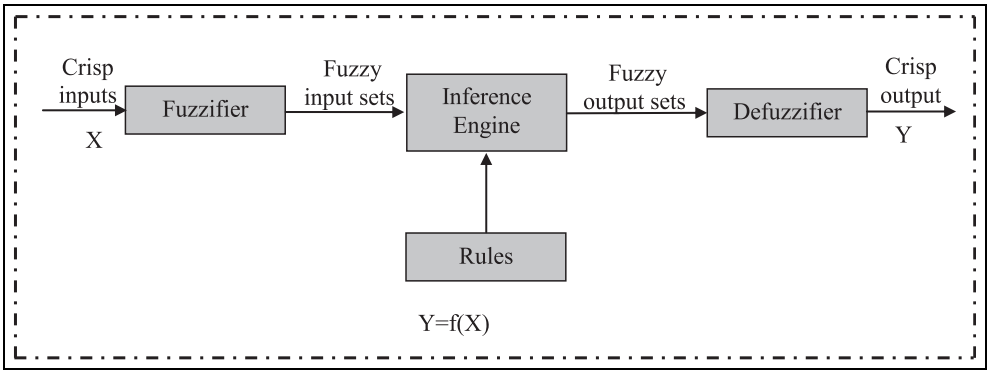

Figure 7. Schematic diagram of classical (type-1) fuzzy logic controller.

are framed based on the expertise knowledge obtained over a time on the system performance. The Figure 7 shows the structural diagram of the well-known conventional fuzzy logic controller (named as type-1 FLC).

Fuzzy logic controllers consist of three processing stages named as fuzzifier, inference engine and a de-fuzzifier. Fuzzifier converts the crisp inputs in to fuzzy sets, with help of the inference engine the fuzzy outputs can be obtained depending upon the fuzzy rules framed based on the membership functions. Finally, de-fuzzifier technique converts these fuzzy output set into a crisp output which is useful for controlling purpose.

Interval type-2 fuzzy logic system

Generally, type-1 fuzzy rules and membership functions (MFs) are defined based on experts' knowledge and experience. However, the uncertainties in actual degree of MFs cannot be modelled once the membership functions have been defined for designing the controller. Quite often the knowledge used to design the type-1 FLC ignore the uncertainties in spread of MFs, rules and membership grade etc. and such system cannot guarantee the optimal performance of the system when it subjected to the disturbances.

From the literature survey, it is found that type-2 fuzzy systems have been successfully applied in many science and engineering applications (Liang et al., 2000a, 2000b). In data process applications, the system with type-2 fuzzy system seems to be more promising method than the type-1 counterpart in processing of noisy data with uncertainties (Jafarzadeh et al., 2012). Type-2 fuzzy system has been applied in decision making (Doctor et al., 2008), survey processing (Lee et al., 2010), solving fuzzy relation equations (Mendel, 2004) and function approximation (Wu and Mendel, 2009) by comparing the performance with its type-1 counterparts. In real world applications which exhibits measurement noise and parameters uncertainties, type-2 fuzzy controllers are better option than type-1 FLC (Hsiao et al., 2008). The controllers with type-2 FLC have shown to have better tracking capability in real-time mobile robots (Martínez et al., 2009). Recently, many power system applications have adopted type-2 FLC as an alternative for handling uncertainties in operating conditions (Khosravi et al., 2011; Flores et al., 2009; Tripathy and Mishra, 2011). The type-2 FLC also offers better performance in automation controller than type-1 FLC (Biglarbegian et al., 2010; Chen et al., 2009; Mendez et al., 2010). The type-2 FLC is also applied in network domain, in order to control of video transmission across the IP networks, where it provided superior video quality compared to existing traditional type-1 FLC counterparts (Jammeh et al., 2008, 2009; Linda et al., 2011). Type-2 FLC applications are also found in health-care and medicine domain due its robust performance than type-1 FLC (Herman et al., 2006). It is believed that a type-2 fuzzy system performs better than type-1 fuzzy system in various areas including communication networks, pattern recognition, mobile communications and renewable energy operated systems. However, in case of type-2 FLC technique the distribution points sits on the FOU is not a uniform (have different values varies from 0 to 1) it leads to more complexity. If all the distribution points sits on the FOU considered as uniform that is, equal to 1 or 0 then this type of fuzzy set named as interval type-2 fuzzy set. The merits of IT-2 FLC are less complexity with robust performance as compared to type-2 FLC. The developed fundamental mathematical background of IT-2 FLC is discussed in the below section.

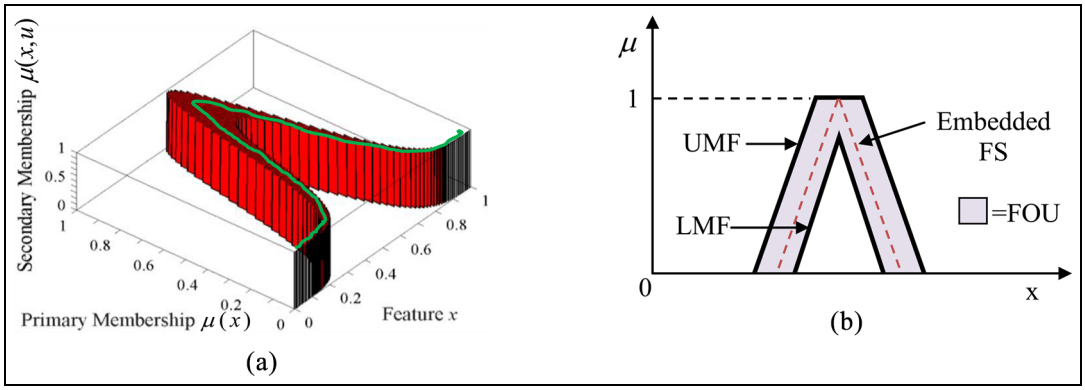

Figure 8. (a) Type-2 FS with FOU and secondary membership grade highlighted and (b) type-2 fuzzy sets with FOU and embedded fuzzy set (FS).

Mathematical background of interval type-2 fuzzy logic. As explained in (Mendel and John, 2002), if all the distribution points which sit on the FOU are uniform, then the resulting type-2 fuzzy sets are called interval type-2 fuzzy sets (Mendel, 1995). These fuzzy sets have less computational complexity with secondary memberships, made either zero or one.

An interval type-2 fuzzy set (denoted $\tilde{A}$) can be characterized as:

$$\tilde{A} = \int_{x \in X} \int_{u \in J_x \subseteq [0,1]} 1/(x,\ u) \tag{7}$$

$$= \int_{x \in X} \left[\int_{u \in J_x \subseteq [0,1]} 1/u \right] \Big/ x \tag{8}$$

$\tilde{A} : X \rightarrow \{[a,\ b] :\ 0 \leqslant a \leqslant b \leqslant 1\}$. Structurally, the membership functions of bothqtype-2 FSs and interval type-2 FSs (IT-2FSs) are three dimensional, with only difference of secondary membership grades of IT-2FSs are either zero or one. In this paper, we choose all the distribution points sits on the FOU is equal to one. Figure 8(a) shows the IT-2 Gaussian membership function in which the secondary membership grade is highlighted (green colour) which consist of all the distribution points equal to 1. The union of all the primary memberships is called the footprint-of-uncertainty (FOU) of $\tilde{A}$ and is shown as the shaded region of Figure 8(b). Uncertainty about $\tilde{A}$ is conveyed by union of all primary memberships, called FOU, can be expressed as:

$$FOU(\tilde{A}) = \cup_{\forall x \in X} J_x = \{(x, u) :\ u \in J_x \subseteq [0,\ 1]\} \tag{9}$$

As shown in Figure 8(b), the FOU of type-2 fuzzy set ($\tilde{A}$) has bounded by two type-1MFs called as lower membership function (LMF) and the upper membership function (UMF). The UMF and LMF are denoted as $\bar{\mu}_{\tilde{A}}(x)$ and $\underline{\mu}_{\tilde{A}}(x)$, respectively, and are defined as follow:

$$\bar{\mu}_{\tilde{A}}(x) = \overline{FOU(\tilde{A})} \qquad \forall_{x \in X} \tag{10}$$

$$\underline{\mu}_{\tilde{A}}(x) = \underline{FOU(\tilde{A})} \qquad \forall_{x \in X} \tag{11}$$

Note that J_x is an interval set; i.e.

$$J_x = \{(x,\ u) : u \in \left[\underline{\mu}_{\tilde{A}}(x),\ \overline{\mu}_{\tilde{A}}(x)\right]\} \tag{12}$$

An embedded fuzzy set (FS) $\tilde{A}_e$ for a continuous universe of discourse X and μ is expressed as

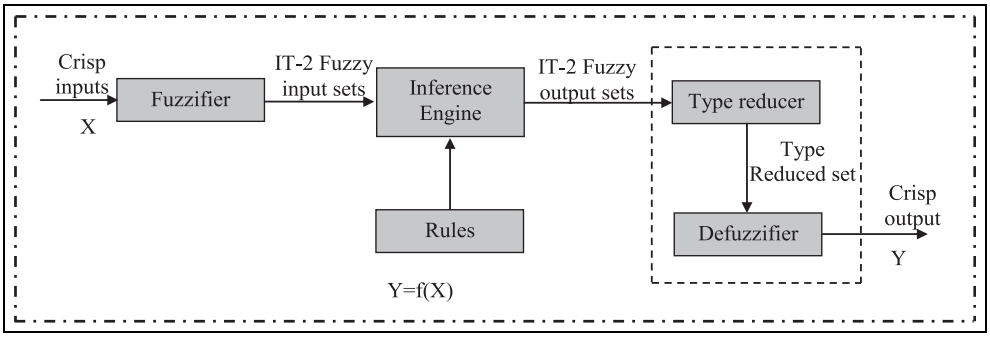

Figure 9. Schematic diagram of type-2 FLC.

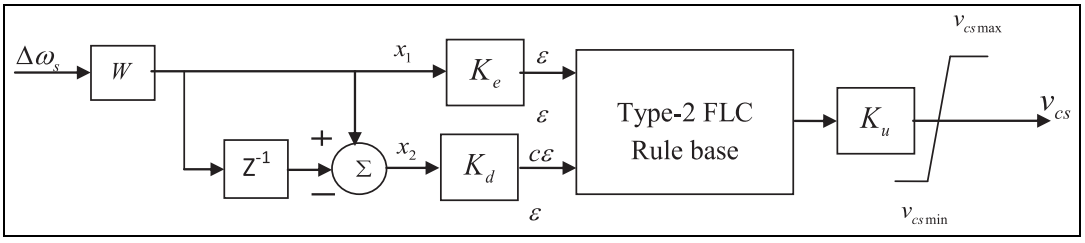

Figure 10. Proposed type-2 fuzzy logic based damping controller.

$$\tilde{A}_e = \int_{x\in X} [1/u]/x, \qquad u \in J_x \tag{13}$$

The set $\tilde{A}_e$ is embedded in $\tilde{A}$ in such a way that the secondary MF is always one at each value of x. A large number of such embedded type-1 fuzzy set (FS) are combined to form the type-2 FS. According to (Mendel 2004), the type-2 FS can be considered as a combination of many differentqtype-1 FSs where each qtype-1 FS is embedded to form the FOU.

Structure of type-2 FLC. Steps involved in design the algorithm of type-2 fuzzy logic controller is shown in the Figure 9. Initially, with help of various membership functions the crisp input is converted to fuzzy inputs using type-2 membership functions of various system parameters so as to account for the uncertainty involved in the expert knowledge. Then using logical operators, a set of fuzzy rules is framed to combine the fuzzy output sets into a single set under the inference mechanism. The output of inference engine is converted to type-1 under type reduction operation and then, the type reduced sets are converted back to crisp value using various defuzzification techniques as done in the type-1 FLC.

The proposed interval type-2 FLC based damping controller is shown in Figure 10. The deviation in SG rotor speed signal is given as input to the type-2 fuzzy damping controller, where initially it passes through the washout filter in order to washout (reject) steady-state components while passing transient components of $\Delta\omega_s$. Later on, it is divided in to two paths: x_1-proportional path and x_2-integral path. Moreover, two input gains K_e and K_d are incorporated to make $\varepsilon = x_1K_e$ and $c\varepsilon = x_2K_d$ usually within a proper range of $[-1, 1]$ for fuzzifier design. Another gain K_u is also employed at the output side of the type-2 fuzzy controller where the type-2 fuzzy logic controller computes the proper output signal v_{cs} through the defuzzification technique. This output signal applied to the STATCOM for damping oscillation control. K_e,K_d and K_u are the gains of the controller which are chosen based on the expert knowledge and experience so as to get satisfactory performance of the type-2 fuzzy controller.

For the fuzzy based damping controller, the two inputs error (ε) and change in error ($c\varepsilon$) are fuzzified using seven Gaussian membership functions as it shows better compensation capabilities. The Gaussian membership function is also used to defuzzify the output fuzzy sets. The fuzzy sets for inputs and output are defined as: Big Negative (BN), Medium Negative (MN), Small Negative (SN), Zero (0), Small Positive (SP), Medium Positive (MP), and Big Positive (BP) and used for the type-1 and type-2 FLCs are shown in Figure 11(a) and (b),

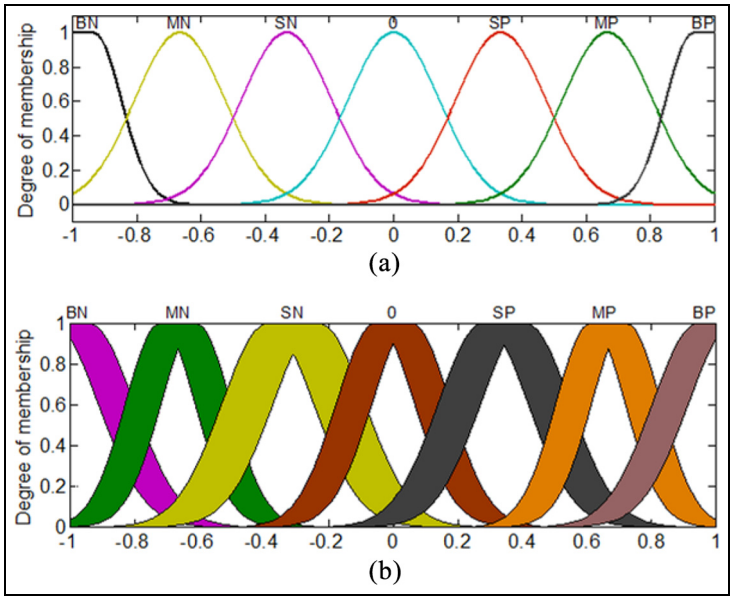

Figure 11. MFs for (a) type-1 FLC and (b) type-2 FLC.

Table 1. Rule base table for v_{cs}.

Change in error ($c\varepsilon$)	Error (ε)						
	BN	MNO	SN	0	SP	MPO	BPO
BPO	0	SP	MPO	BPO	BPO	BPO	BPO
MPO	SN	0	SPO	MP	BPO	BPO	BPO
SPO	MN	SNO	0	SP	MP	BP	BPO
0	BNO	MNO	SN	0	SP	MP	BPO
SNO	BNO	BNO	MNO	SN	0	SP	MPO
MNO	BNO	BNO	BNO	MNO	SN	0	SP
BNO	BNO	BNO	BNO	BN	MNO	SNO	0

respectively. The maximum and minimum values of the universe of discourse for all inputs and outputs are -1 to + 1. The fuzzy mapping of input variable to output is formed with help of the IF-THEN rules framed as:

IF: ε is A_i and $c\varepsilon$ is B_i THEN $v_{cs} = C_i$

Where ε and $c\varepsilon$ are inputs and A_i and B_i are the fuzzy sets, C_i is the output within the fuzzy range, v_{cs} is designed parameter for the output of fuzzy. Similarly, 49 rules are formed as shown in Table 1.

Real time simulations

OPAL-RT digital simulator has considered to carry the real time simulation of the studied system. The RT-lab which is fully integrated with MATLAB/Simulink®, provides the flexibility and scalability to achieve the most complex real-time simulation applications in the power systems, power electronics, automotive, aerospace and industries (Jalili-Marandi et.al., 2009; Mikkili and Panda, 2013; Mikkili et al., 2015; Venne et al., 2010). The proposed interval type-2 fuzzy logic algorithm for damping controller is modelled by real time simulator using SimPowerSystem blockset and ARTEMiS plug in. The RT-lab can separate a complex system into simple subsystems and performs parallel operation in multiple cores with highly accurate and lower cost real-time execution. The real time simulation is developed to examine the applicability of the proposed fuzzy technique as prototype

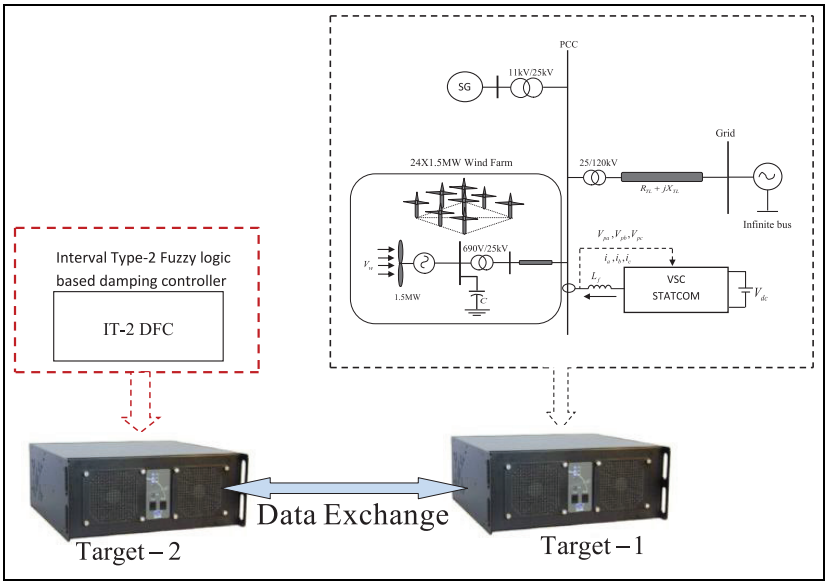

Figure 12. Wind power system model for real time simulation, implemented using RT-Lab in HIL application.

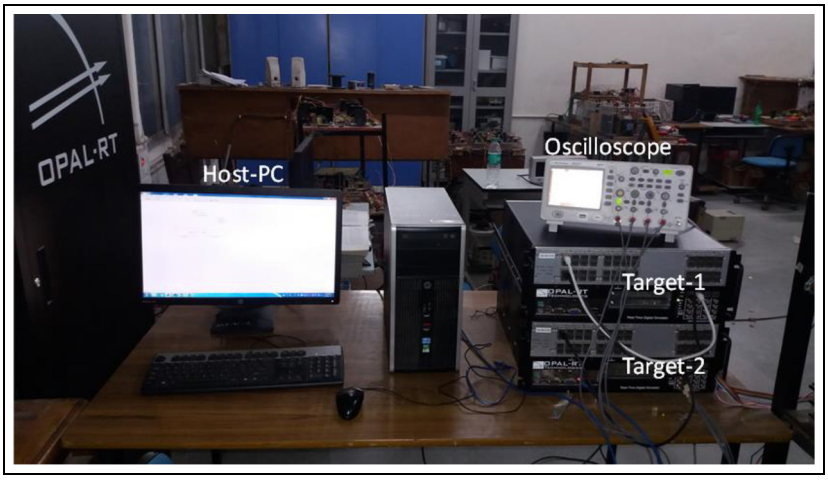

Figure 13. Real time digital simulator laboratory setup.

controller, which is essential stage before real time implementation. The real time simulator performs two main functions named as: rapid control prototype (RCP) and hardware in loop (HIL). The RCP realization is employed to implement the proposed interval type-2 fuzzy logic controller in order to mimics real time damping controller. The HIL application is required to investigate the proposed controller as RCP controller when it connected to a wind integrated power system and realized in real time. Figure 12 shows the wind power system test model used in hardware in loop application. The RT-Lab simulator consists of two processors (targets). To realize the HIL configuration, a typical wind power system is implemented in Target-1 where the wind farm, SG and STATCOM are assigned to separate cores to perform parallel computation. The proposed interval type-2 fuzzy logic based damping controller (IT-2 DFC) algorithm is implemented in Target-2. Both targets exchange data in real time environment to examine the proposed fuzzy controller as prototype controller.

The real time digital simulation laboratory setup is as shown in Figure 13; it consists of host personal computers (Host-PC), two targets (real time digital simulators) and oscilloscope. The simulator each employed here is OP5600 with one processor and fours 3.33-GHz dedicated cores to perform parallel computations. The sampling time used to realize the system is $50\mu s$. The digital oscilloscope is also employed to observe the real time results.

More detailed study about OPALRT and HIL applications are suggested in RT-LAB (2019) and Craciun et al. (2014).

Results and discussions

In order to observe the improvement in performance of the proposed interval type-2 fuzzy algorithm, the real time simulations are developed for three different scenarios such as:

(i) Studied wind power system-without damping controller
(ii) Studied wind power system-with type-1 FLC designed damping controller
(iii) Studied wind power system-with interval type-2 FLC designed damping controller

To examine the effective damping characteristics contributed by the IT-2 FLC based damping controller of STATCOM, different uncertainty conditions occurs in the studied system such as a noise wind speed disturbance and network faults are considered.

Wind speed disturbance

The dynamic responses of the studied wind power system subjected to a wind speed disturbances are as illustrated in Figure 14(b) to (e). The wind speed disturbance considered in this paper is as shown in Figure 14(a). Figure 14(b) shows the active power generated by the wind farm, as there is no damping controller it follows the wind speed disturbances and, if these output power oscillations enter in to the power network leads to grid frequency problems therefore, damping controllers are necessary to damp these power oscillations. The damping controller designed with type-1 and type-2 FLCs offered better results as shown in Figure 14(b), but the damping controller designed with type-2 FLC contributes effective damping characteristics to the studied system. Figure 14(c) reveals that due to wind speed disturbances/variations, rotor speed of wind turbine produced similar variations. But these variations are damped out more effectively by the proposed damping controller.

Figure 14(d) represents the magnitude of the PCC (point of common coupling) voltage obtained with three different scenarios. It is observed that the voltage fluctuating severely with an absence of damping controller. This condition further results in voltage fluctuations at the PCC in a reasonable range and causes flicker problems. It (voltage flicker) is a major limiting factor with the connection of the wind turbines into weak grids, where the wind penetration level is very high. When the damping controller designed with different control techniques (type-1 and type-2 FLCs) are employed, the voltage fluctuations are suppressed drastically but, the effective damping characteristics is achieved with proposed type-2 fuzzy algorithm based damping controller. Similarly, Figure 14(e) illustrates the reactive power exchange of the wind farm with PCC. It is clearly observed that the oscillations due to the wind speed disturbances are more effectively reduced by the proposed damping controller.

The controller error signal generated by the type-1 and type-2 FLCs are captured in digital oscilloscope as shown in Figure 15(a) and (b). The time division considered in the oscilloscope is 25s per division. Figure 15(a) shows the type-1 FLC controller error output it producing high oscillations where as Figure 15(b) represents the type-2 FLC whose controller error signal almost lasted oscillations throughout the wind speed disturbances.

Network faults

To investigate the contribution of the proposed damping controller, this section uses the nonlinear simulation test system which is shown in Figure 1. Three cases have been considered to study the effectiveness of the type-1 and type-2 FLC based damping controllers as follows:

Case 1: Three-line-to-ground fault (LLG)
Case 2: Two-line-to-ground fault (LLG)
Case 3: Single-line-to = ground fault (LG)

In all the cases the faults have been occurs at t = 10sec and cleared at t = 10.05sec. The operating wind speed is assumed to be constant at 14m/sec. The simulation results of studied system are obtained for three different scenarios such as STATCOM-without damping controller, STATCOM with type-1 FLC based damping controller and STATCOM with type-2 FLC based damping controller.

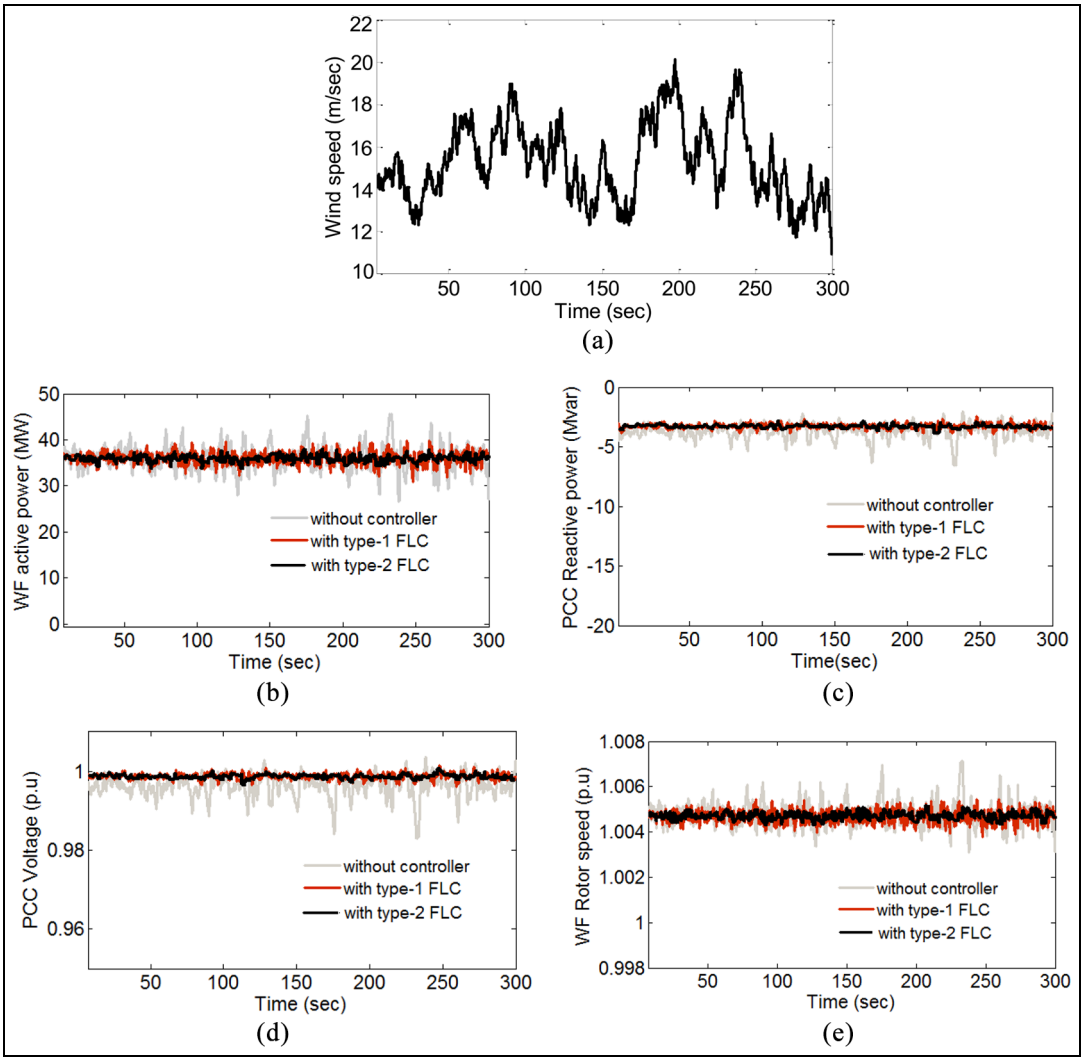

Figure 14. Dynamic response of the studied system subjected to a noise wind speed disturbances: (a) wind speed, (b) WF active output power, (c) reactive power exchange at the PCC, (d) PCC Voltage, and (e) induction generator rotor speed.

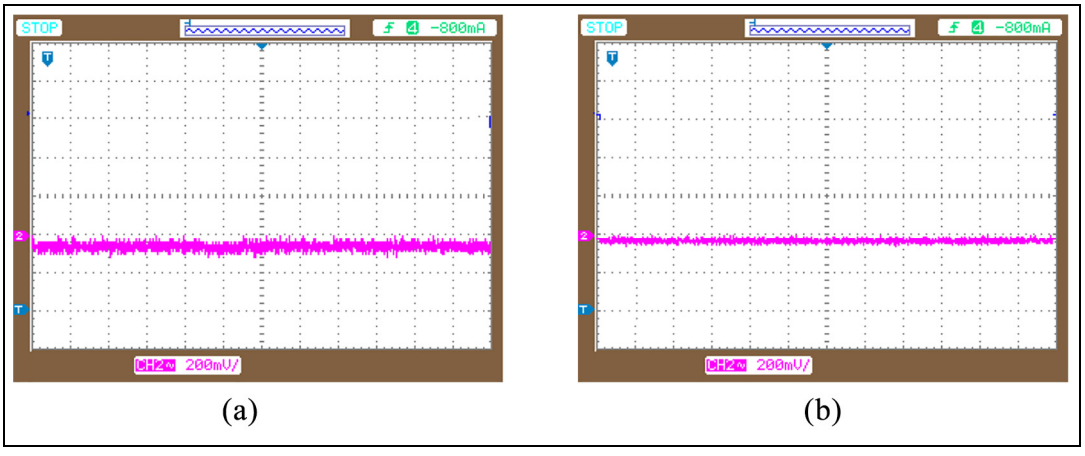

Figure 15. Control error signals: (a) with type-1 FLC and (b) with type-2 FLC.

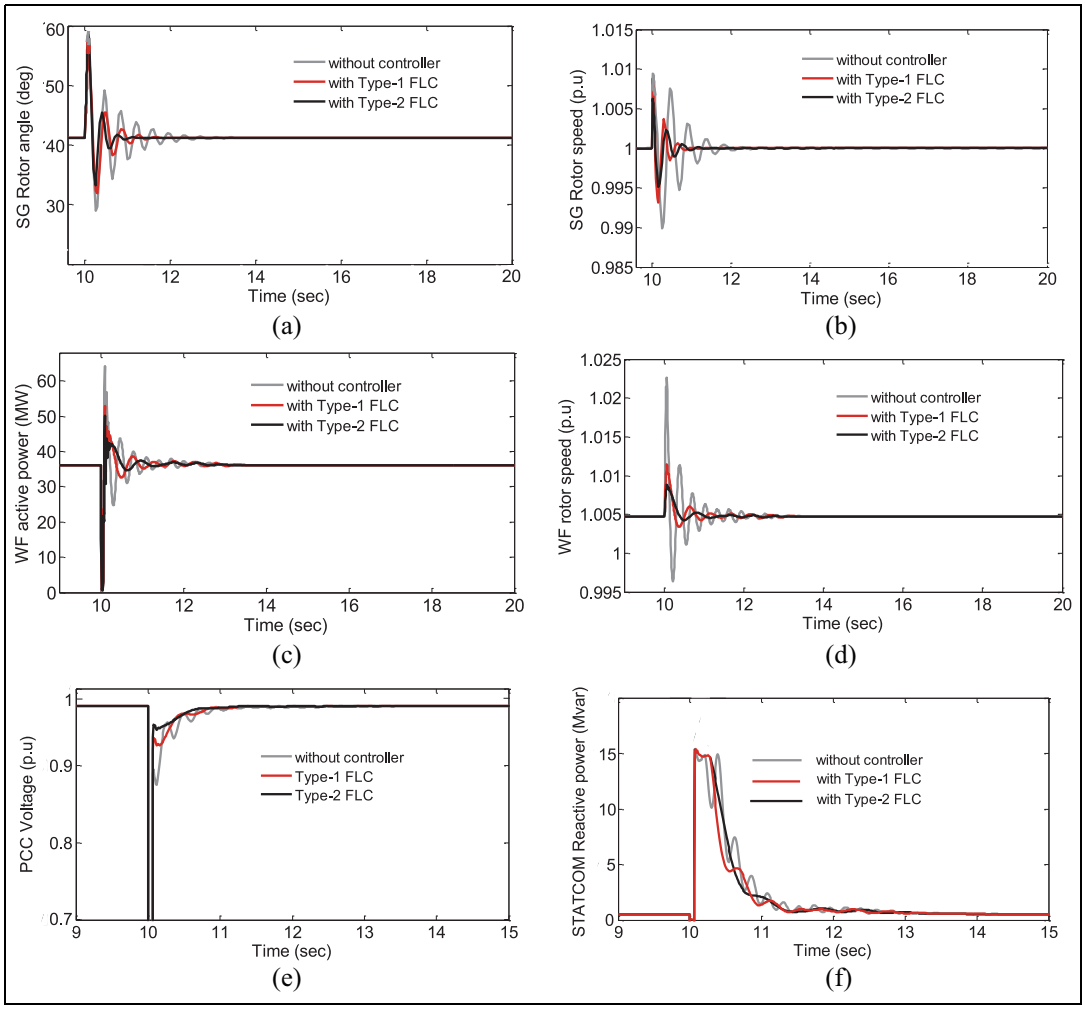

Figure 16. Responses of the studied system under three-line-to-ground fault: (a) SG rotor angle, (b) SG rotor speed, (c) wind farm active power, (d) wind farm generator rotor speed, (e) voltage at the PCC, and (f) reactive power supplied by the STATCOM.

Figure 16(a) to (f) shows the wind integrated power system behaviour under the three phase short circuit fault (case 1). This figure plots the comparative transient responses of the system with STATCOM-without damping controller (gray lines), STATCOM-with designed type-1 FLC damping controller (red lines) and STATCOM-with proposed type-2 FLC damping controller (black lines). The real power oscillation in wind farm is shown in Figure 16(c), the STATCOM with proposed type-2 FLC based damping controller offers better damping effect and quickly return to steady state around 0.5sec. The dynamic response of the SG and IG rotor speed are shown in Figure 16(b) and (d), respectively. It can found that the proposed controller has faster convergence rate than other scenarios and recover more quickly to steady state value. Figure 16(a) shows the rotor angle of the SG where proposed controller exhibits better damping results than STATCOM-without damping controller and with type-1 FLC based damping controller. This type of fault also leads to fluctuations in voltage as shown in Figure 16(e), thus voltage stability is also required. Figure 16(e) shows that STATCOM with type-2 FLC based damping controller improve the transient stability and effective voltage recovery is achieved. The reactive power generation of the STATCOM without damping controller and with damping controller (designed with type-1 and type-2 FLCs) are shown in Figure 16(f).

The performance of the proposed controller is also estimated using absolute maximum deviations in terms of performance indices. It is employed to obtain the index values for all the quantities such as SG rotor-angle, SG rotor-speed, WF active-power and WF rotor-speed of the studied system and are listed in Table 2. If absolute maximum deviation is small, the generated fluctuation in the wind farm is small; as a result, the studied system exhibits good performance. It is observed from the Table 2 that the type-2 FLC based damping controller

Table 2. Maximum deviation in the quantities of the studied system under the 3LG fault disturbance.

Quantities	Studied system without damping controller	Studied system with type-1 FLC damping controller	Studied system with type-2 FLC damping controller
SG rotor angle	3.9514	3.9016	3.8801
SG rotor speed	0.0021	0.0013	0.0011
WF active power	4.1618	4.1204	4.1003
WF rotor speed	0.0028	0.0017	0.0014

Table 3. Maximum deviation in the quantities of the studied system under the 2LG fault disturbance.

Quantities	Studied system without damping controller	Studied system with type-1 FLC damping controller	Studied system with type-2 FLC damping controller
SG rotor angle	3.5853	3.5058	3.3811
SG rotor speed	0.0019	0.0013	0.0009
WF active power	3.7957	3.7274	3.5810
WF rotor speed	0.0026	0.0014	0.0012

Table 4. Maximum deviation in the quantities of the studied system under the LG fault disturbance.

Quantities	Studied system without damping controller	Studied system with type-1 FLC damping controller	Studied system with type-2 FLC damping controller
SG rotor angle	2.2851	2.2053	2.0811
SG rotor speed	0.0007	0.00055	0.00043
WF active power	3.5847	3.5629	3.5412
WF rotor speed	0.0014	0.0008	0.0003

produced smaller absolute maximum deviations when wind farm subjected to LLLG fault as compared to the other two scenarios (without damping controller and type-1 FLC controller). Therefore, the proposed damping controller with STATCOM enhances the wind farm performance.

Figure 17(a) to (f) shows the transient behaviour of the studied system with double line to ground fault (case 2). Though, this type of fault is less severe compared to three phase short circuit faults, it has negative impact on the system. From the simulation results it is observed that STATCOM with external damping controller designed using type-2 FLC offers better damping effect and fast convergence rate than other two scenarios. Similarly, a performance index for this type of fault is also obtained and Table 3 provided the maximum parameters deviation for all types of scenarios. It showed that proposed damping controller exhibits lesser parameters deviations compared to without and with type-1 FLC damping controllers.

The system transient behaviour with single to ground fault (case 3) with different scenarios is shown in Figure 18(a) to (f). Though, this type of fault is lesser severe compared to double line to ground and three line to ground faults, but it is most frequently occurs and therefore, need to investigate its impact on the system. From the simulation results it is examined that the fluctuations occur due to LG fault are effectively damped out by the proposed controller. The maximum deviation of the system parameters with three different scenarios are incorporated in the Table 4. In this case as well proposed controller offers lesser deviations in the parameters. As a result proposed controller offers good dynamic performance.

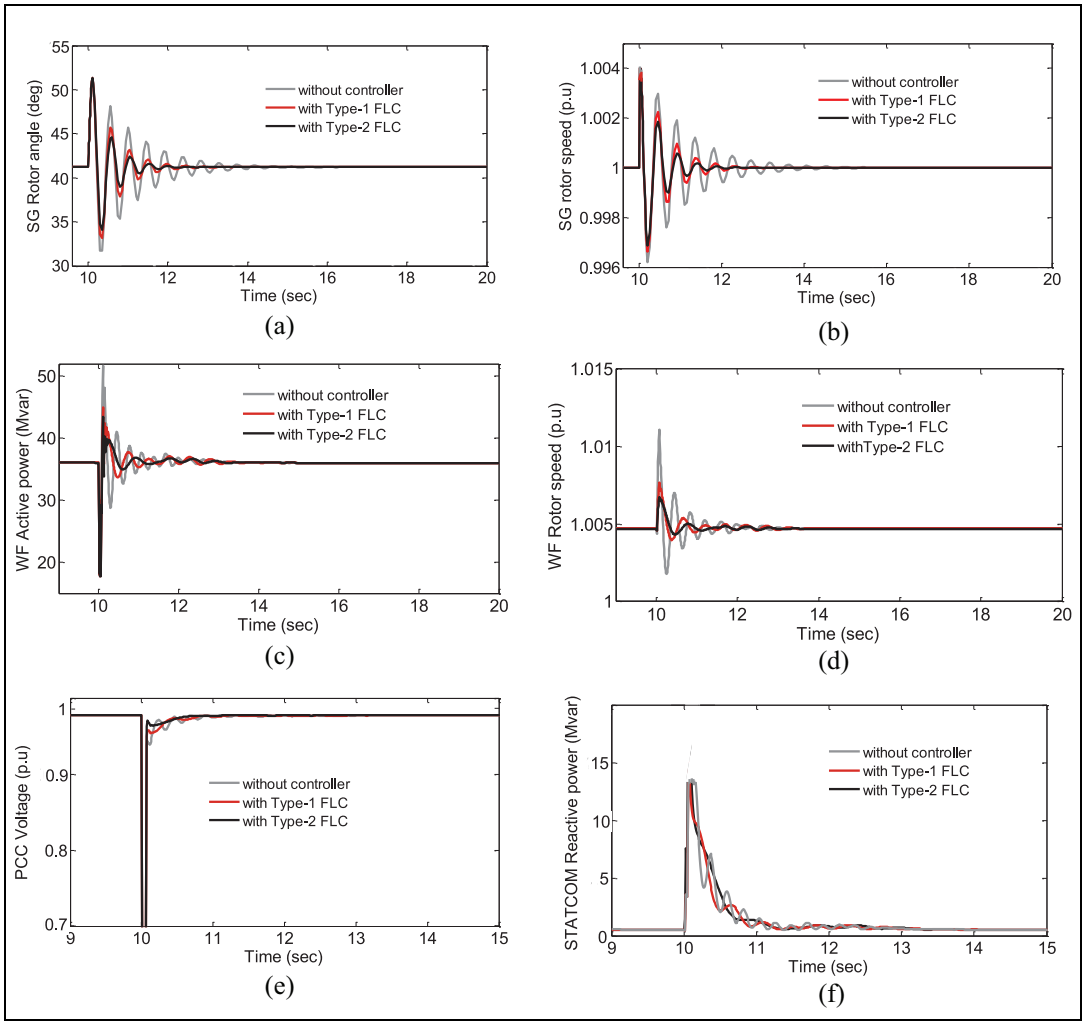

Figure 17. Responses of the studied system under two-line-to-ground fault: (a) SG rotor angle, (b) SG rotor speed, (c) wind farm active power, (d) wind farm generator rotor speed, (e) voltage at the PCC, and (f) reactive power supplied by the STATCOM.

The controllers' error input are also observed in the digital oscilloscope as shown in Figure 19(a) and (b) respectively, for type-1 FLC and type-2 FLC. At the time of fault, the controller error output increases in order to bring the generator parameters at normal level. It is observed that the error signal generated by the proposed method is lasted few seconds compared to that of type-1 FLC and shows that the proposed method is able to improve the performance of the system subjected to network faults.

Figure 20(a) and (b) shows the control surfaces formed by the type-1 and type-2 FLCs, respectively. It is observed from Figure 20(b) that as its control surface is formed with large number of embedded type-1 FSs, the proposed type-2 controller surface is very smooth as compared to type-1 FLC shown in Figure 20(a). This smooth surface is less sensitive to disturbances and therefore, its effect is clearly visible on the responses of the studied system as shown in Figures 14, 16, 17 and 18.

Conclusions

Taking the consideration of limited non-renewable energy resources available and with ever increasing electricity need, it has become absolute necessity to integrate wind farms in to the grid. Handling the uncertainties in the wind speed and the grid disturbances is a major challenge to the wind power system to fulfil the modern grid code requirements. The third dimensional membership function and FOU present in interval type-2 fuzzy logic technique offers additional degree of freedom to overcome the uncertainties during formation of MFs and rules.

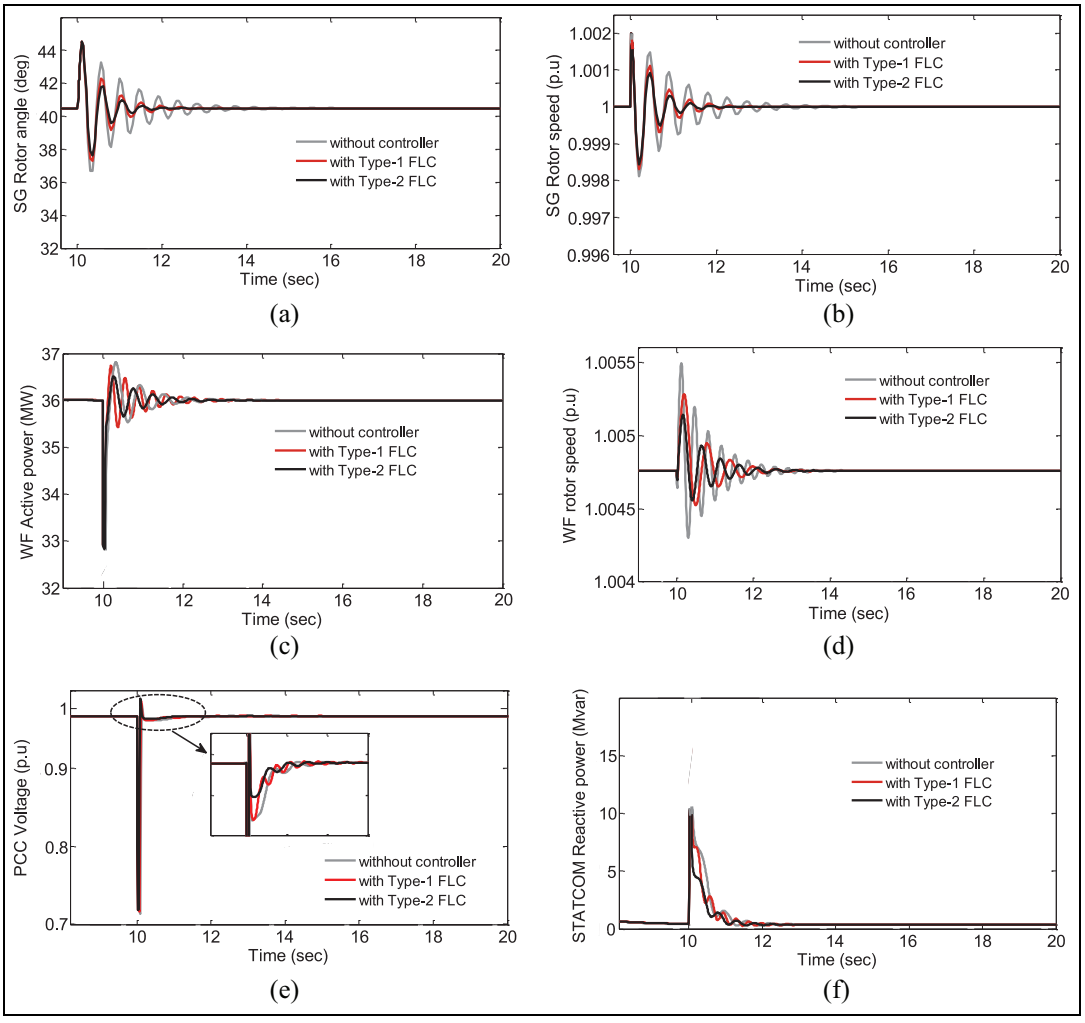

Figure 18. Responses of the studied system under single-line-to-ground fault: (a) SG rotor angle, (b) SG rotor speed, (c) wind farm active power, (d) wind farm generator rotor speed, (e) voltage at the PCC, and (f) reactive power supplied by the STATCOM.

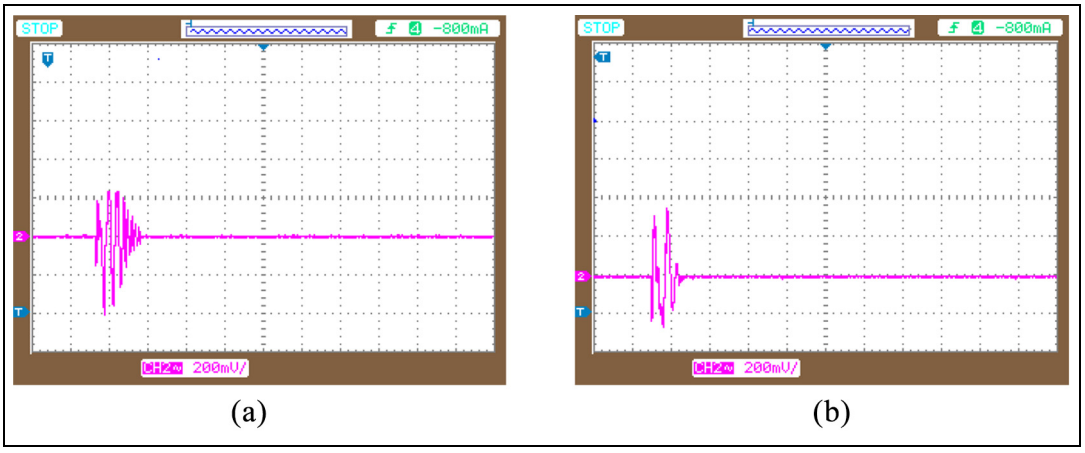

Figure 19. Control error signals: (a) with type-1 FLC and (b) with type-2 FLC.

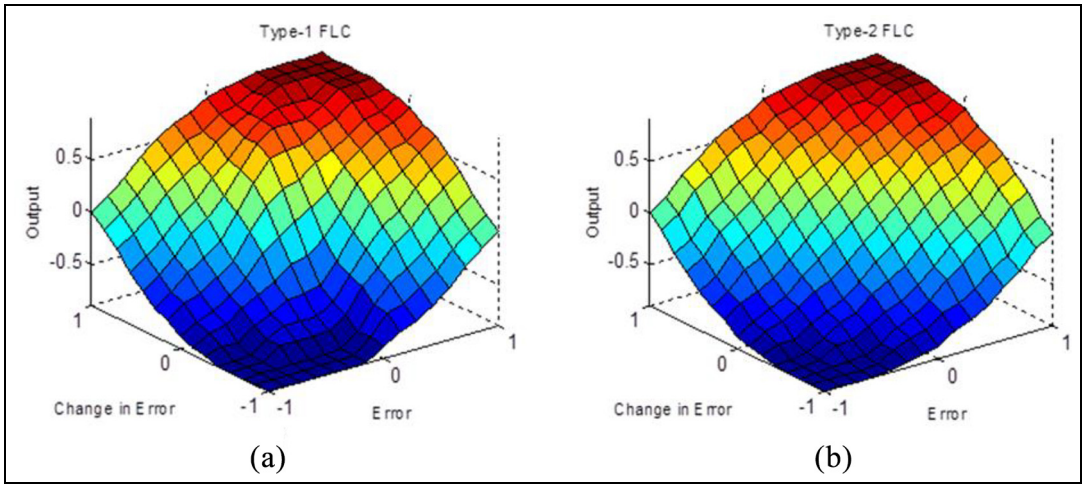

Figure 20. Control surfaces: (a) type-1 FLC and (b) type-2 FLC.

Therefore, in this paper, an intervalstype-2 fuzzy logic based damping controller which includes at STATCOM control block is proposed, and implemented through hardware in loop configuration using OPAL-RT laboratory. Different scenarios are executed such as system without damping controller, with damping controller designed by using type-1 and type-2 FLCs. It is observed that STATCOM equipped with proposed IT-2 FLC based damping controller suppressed the inherent fluctuations of the studied system effectively, and thus enhances the stability. Finally, it is concluded that real-time implementation of proposed controller as a rapid control prototyping is offers satisfactory results and thereby applicable to practical system as well.

Declaration of conflicting interests

The author declared no potential conflicts of interest with respect to the research, authorship, and/or publication of this article.

Funding

The author received no financial support for the research, authorship, and/or publication of this article.

ORCID iD

Kanasottu Anil Naik https://orcid.org/0000-0002-3321-5097

References

Ackermann T (2005) *Wind Power in Power System*. Hoboken, NJ: John Wiley & Sons.

Biglarbegian M, Melek WW and Mendel JM (2010) Design of novel interval type-2 fuzzy controllers for modular and reconfigurable robots: Theory and experiments. *IEEE Trans Ind Electron* 58(4): 1371–1384.

Causebrook A, Atkinson DJ and Jack AG (2007) Fault ride-through of large wind farms using series dynamic braking resistors. *IEEE Trans Power Syst* 22(3): 966–975.

Chen WL, Liang WG and Gau HS (2009) Design of a mode decoupling STATCOM for voltage control of wind-driven induction generator systems. *IEEE Trans Power Deliv* 25(3): 1758–1767.

Craciun O, Florescu A, Munteanu I, et al. (2014) Hardware-in-the-loop simulation applied to protection devices testing. *Int J Electr Power Energy Syst* 54: 55–64.

Doctor F, Hagras H, Roberts D, et al. (2008) A type-2 fuzzy based system for handling the uncertainties in group decisions for ranking job applicants within human resources systems. In: *2008 IEEE international conference on fuzzy systems (IEEE World congress on computational intelligence)*, Hong Kong, China, 1–6 June 2008, pp.481–488. New York, NY: IEEE.

Edrisian A, Goudarzi A, Davidson IE, et al. (2015) Enhancing SCIG-based wind turbine generator performance through reactive power control. In: *Clemson university power systems conference (PSC)*, Clemson: IEEE, 2015, pp.1–8.

Flores WC, Mombello E, Jardini JA, et al. (2009) Fuzzy risk index for power transformer failures due to external short-circuits. *Electr Power Syst Res* 79(4): 539–549.

Ghazi R and Aliabadi H (2010) Stability improvement of wind farms with fixed-speed turbine generators using braking resistors. In: *45th international universities power engineering conference UPEC*, Cardiff: IEEE, 2010, pp.1–5.
Hagras H and Wagner C (2012) Towards the wide spread use of type-2 fuzzy logic systems in real world applications. In: *IEEE computational intelligence magazine*, August 2012, vol. 7, pp.14–24. New York: IEEE.
Herman P, Prasad G and McGinnity TM (2006) Investigation of the type-2 fuzzy logic approach to classification in an EEG-based brain-computer interface. In: *2005 IEEE engineering in medicine and biology 27th annual conference*, January 2006, pp.5354–5357. New York, NY: IEEE.
Herman P, Prasad G and McGinnity TM (2008) Design and on-line evaluation of type-2 fuzzy logic system-based framework for handling uncertainties in BCI classification. In: *2008 30th annual international conference of the IEEE engineering in medicine and biology society*, August 2008, pp.4242–4245. New York, NY: IEEE.
Hsiao MY, Li THS, Lee JZ, et al. (2008) Design of interval type-2 fuzzy sliding-mode controller. *Inf Sci* 178(6): 1696–1716.
Jafarzadeh S, Fadali MS and Etezadi-Amoli M (2012) Fuzzy type-1 and type-2 TSK modeling with application to solar power prediction. In: *2012 IEEE power and energy society general meeting*, San Diego, CA, 22–26 July 2012, pp.1–6. New York, NY: IEEE.
Jalili-Marandi V, Pak LF and Dinavahi V (2009) Real-time simulation of grid-connected wind farms using physical aggregation. *IEEE Trans Ind Electron* 57(9): 3010–3021.
Jammeh E, Fleury M and Ghanbari M (2008) Fuzzy-logic congestion control of transcoded video streaming without packet loss feedback. *IEEE Trans Circuits Syst Video Technol* 18(3): 387–393.
Jammeh EA, Fleury M, Wagner C, et al. (2009) Interval type-2 fuzzy logic congestion control for video streaming across IP networks. *IEEE Trans Fuzzy Syst* 17(5): 1123–1142.
Jauch C, Cronin T, Sorensen P, et al. (2007) A fuzzy logic pitch angle controller for power system stabilization. *Wind Energy* 10(1): 19–30.
Khosravi A, Nahavandi S and Creighton D (2011) Short term load forecasting using interval type-2 fuzzy logic systems. In: *2011 IEEE international conference on fuzzy systems (FUZZ-IEEE 2011)*, June 2011, pp.502–508. New York, NY: IEEE.
Lee CS, Wang MH and Hagras H (2010) A type-2 fuzzy ontology and its application to personal diabetic-diet recommendation. *IEEE Trans Fuzzy Syst* 18(2): 374–395.
Liang Q and Mendel JM (2000a) Equalization of nonlinear time-varying channels using type-2 fuzzy adaptive filters. *IEEE Trans Fuzzy Syst* 8: 551–563.
Liang Q and Mendel JM (2000b) Overcoming time-varying co-channel interference using type-2 fuzzy adaptive filters. *IEEE Trans Circuits Syst II Analog Digit Signal Process* 47(12): 1419–1428.
Linda O, Manic M, Alves-Foss J, et al. (2011) Towards resilient critical infrastructures: Application of type-2 fuzzy logic in embedded network security cyber sensor. In: *2011 4th international symposium on resilient control systems*, August 2011, pp.26–32. New York, NY: IEEE.
Martínez R, Castillo O and Aguilar LT (2009) Optimization of interval type-2 fuzzy logic controllers for a perturbed autonomous wheeled mobile robot using genetic algorithms. *Inf Sci* 179(13): 2158–2174.
Mendel JM (1995) Fuzzy logic systems for engineering: A tutorial. *Proc IEEE* 83(3): 345–377.
Mendel JM (1999) Computing with words when words can mean different things to different people. In: *Proceedings of third international ICSC symposium on fuzzy logic and applications*, pp.1–7. Rochester, NY: Rochester Institute of Technology.
Mendel JM (2004) Computing derivatives in interval type-2 fuzzy logic systems. *IEEE Trans Fuzzy Syst* 12(1): 84–98.
Mendel JM and John RIB (2002) Type-2 fuzzy sets made simple. *IEEE Trans Fuzzy Syst* 10(2): 117–127.
Mendel JM, John RI and Liu F (2006) Interval type-2 fuzzy logic systems made simple. *IEEE Trans Fuzzy Syst* 14: 808–821.
Mendez GM, Leduc-Lezama L, Colas R, et al. (2010) Modelling and control of coiling entry temperature using interval type-2 fuzzy logic systems. *Ironmaking Steelmaking* 37(2): 126–134.
Mikkili S and Panda AK (2013) Types-1 and -2 fuzzy logic controllers-based shunt active filter Id–Iq control strategy with different fuzzy membership functions for power quality improvement using RTDS hardware. *IET Power Electron* 6(4): 818–833.
Mikkili S, Panda AK and Prattipati J (2015) Review of real-time simulator and the steps involved for implementation of a model from MATLAB/SIMULINK to real-time. *J Inst Eng B* 96(2): 176–196.
Molinas M, Suul JA and Undeland T (2008) Low voltage ride through of wind farms with cage generators: STATCOM versus SVC. *IEEE Trans Power Electron* 23(3): 1104–1117.
Ou R, Xiao XY, Zou ZC, et al. (2015) Application of SFCL to improve the transient voltage stability of grid-connected wind farm with DFIG during grid faults. In: *IEEE international conference on applied superconductivity and electromagnetic devices (ASEMD)*, Shanghai, China, 2015, pp.240–241. New York, NY: IEEE.
Ou TC, Lu KH and Huang CJ (2017) Improvement of transient stability in a hybrid power multi-system using a designed NIDC (Novel Intelligent Damping Controller). *Energies* 10(4): 488.
Qilian L and Mendel JM (2000) Interval type-2 fuzzy logic systems: Theory design. *IEEE Trans Fuzzy Syst* 8: 535–550.
Ramirez D, Martinez S, Blazquez F, et al. (2012) Use of STATCOM in wind farms with fixed-speed generators for grid code compliance. *Renew Energy* 37(1): 202–212.
RT-LAB (2019) RT-LAB Version 10.7.0.*361 User Guide, Opal-RT*. Uttarakhand, India: IIT Roorkee.

Sheikh MRI, Mondol N and Eva F (2012) Stabilization of wind generator by PWM-VSC controlled SMES. In: *2nd international conference on the developments in renewable energy technology (ICDRET 2012)*, Dhaka: IEEE. pp.1–5.
Singh B, Murthy SS and Gupta S (2006) STATCOM-based voltage regulator for self-excited induction generator feeding nonlinear loads. *IEEE Trans Ind Electron* 53(5): 1437–1452.
Singh G, Lentijo S and Sundaram K (2019a) The impact of the converter on the reliability of a wind turbine generator. In: *ASME 2019 power conference*, Salt Lake City, Utah, USA, 15–18 July 2019 Salt Lake City: ASME. pp.1–6. ASME.
Singh G, Matuonto M and Sundaram K (2019b) Impact of imbalanced wind turbine generator cooling on reliability. In: *10th international renewable energy congress (IREC)*, Sousse, Tunisia, 26–28 March 2019, pp.1–6. New York, NY: IEEE.
Singh G, Saleh A, Amos J, et al. (2018) Ic6a1a6 vs. ic3a1 squirrel cage induction generator cooling configuration challenges and advantages for wind turbine application. In: *12th international conference on energy sustainability and the ASME 2018 nuclear forum*, Lake Buena Vista, FL, USA, 24–28 June 2018, pp.1–7. Lake Buena Vista: ASME.
Singh G and Sundaram K (2020) Manufacturing deformation impact on the performance of electrical generator for the wind turbine application. *Wind Engineering* 12: 1–13.
Singh G and Sundaram K (2021) Methods to improve wind turbine generator bearing temperature imbalance for onshore wind turbines. *Wind Engineering* 13: 1–10.
Singh G, Sundaram K and Matuonto M (2020) A solution to reduce overheating and increase wind turbine systems availability. *Wind Engineering* 45(3): 491–504.
Sravanthi P, Rani KR, Amarnath J, et al. (2014) Critical clearing time and transient stability analysis of SCIG based wind farm with STATCOM. In: *International conference on smart electric grid (ISEG)*, Guntur, India, 2014, pp.1–8. Guntur: IEEE.
Tan O, Paap GC and Kolluru MS (1993) Thyristor-controlled voltage regulators for critical induction motor loads during voltage disturbances. *IEEE Trans Energy Convers* 8(1): 100–106.
The Global Wind Energy Council Belgium (2020) Available at: https://gwec.net.
The Wind power (2019) Available at: https://www.thewindpower.net.
Thet AK and Saitoh H (2009) Pitch control for improving the low-voltage ride-through of wind farm. In: *Transmission & distribution conference & exposition: Asia and Pacific*, Seoul, South Korea, 2009, pp.1–4. Seoul: IEEE.
Tripathy M and Mishra S (2011) Interval type-2-based thyristor controlled series capacitor to improve power system stability. *IET Gener Transm Distrib* 5(2): 209–222.
Truong DN (2016) STATCOM based fuzzy logic damping controller for improving dynamic stability of a grid connected wind power system. In: *IEEE international conference system science and engineering (ICSSE)*, National Chi Nan University, Puli, Taiwan, 7–9 July 2016, pp.1–4. New York, NY: IEEE.
Venne P, Paquin JN and Belanger J (2010) The what, where and why of real-time simulation. In: *Proceedings of the power and energy society general meeting*, Minneapolis, MN, 1–4 October 2010, pp.37–49. USA: PES.
Vimalraj M, Alex B and Tamilarasi M (2014) StatCom control for voltage stability improvement at a fixed speed wind farm under unbalanced faults. In: *International conference on information communication and embedded systems (ICICES2014)*, Chennai, India, 27–28 February 2014, pp.1–6. New York, NY: IEEE.
Wang L and Truong DN (2013) Stability enhancement of DFIG-based offshore wind farm fed to a multi-machine system using a STATCOM. *IEEE Trans Power Syst* 28(3): 2882–2889.
Wu D and Mendel JM (2009) A comparative study of ranking methods, similarity measures and uncertainty measures for interval type-2 fuzzy sets. *Inf Sci* 179(8): 1169–1192.
Zadeh LA (1965) Fuzzy sets. *Inf Control* 8: 338–353.

Appendix

Wind turbine parameters:

Rated power = 1.5 MW; Rotor diameter = 64 m; Cut-in wind speed (V_{wCI}) = 4 m/sec; Cut-out wind speed (V_R) = 25 m/sec; Rated wind speed (V_{wR}) = 14 m/sec; Number of blades = 3.

IG generator parameters:

$$P_{\text{rated}} = 1.5\text{MW}; V_{\text{rated}} = 0.69\text{kV}; R_s = 0.004843 \text{ p.u}, R_r = 0.004377 \text{ p.u}; L_s = 0.1248 \text{ p.u}, L_r = 0.1791\text{p.u};$$
$$L_m = 6.77 \text{ p.u}, H = 5.04\text{s}; \text{C} = 200 \text{ kVAR}$$

Synchronous generator parameters:

$$S_{rated} = 100 \text{ MVA}; V_{rated} = 11\text{kV}; \text{Inertia } H = 3.5s; r_a = 0.003\text{p.u}, x_l = 0.15\text{p.u}; x_d = 1.81\text{p.u}, x_d^{'} = 0.30\text{p.u}; x_d^{''} = 0.23\text{p.u}, x_q = 1.76\text{p.u}; x_q^{'} = 0.65\text{p.u}, x_q^{''} = 0.25\text{p.u}; T_{d0}^{'} = 8.00\text{s}, T_{d0}^{''} = 0.03\text{s}; T_{q0}^{'} = 1.00\text{s}, T_{q0}^{''} = 0.07\text{s}.$$

STATCOM:

$$VA = 15\text{MVA}; V_{dc} = 4000\text{V}; L_f = 0.5\text{mH}; R_f = 0.25\Omega; C_{dc} = 3600\mu\text{F}; K_{Pac} = 5, K_{Iac} = 100, K_{Pdc}0.001 \text{ and } K_{Idc} = 0.2$$